Supporting Information for

One-dimension coaxial cable-like MWCNTs/Sn_4P_3@C as anode materials with long-term durability for lithium ion batteries

Shuting Sun [a], Ruhong Li [a], Wenhui Wang*[b1] , Deying Mu [a], Jianchao Liu [a], Tianrui Chen [a], Shuang Tian [c], Weimin Zhu [d] and Changsong Dai*[a2]

[a] MIIT Key Laboratory of Critical Materials Technology for New Energy Conversion and Storage, School of Chemistry and Chemical Engineering, Harbin Institute of Technology, Harbin, 150001, China

[b] School of Civil and Environmental Engineering, Harbin Institute of Technology, Shenzhen, 518055, China

[c] Ningbo Institute of Materials Technology & Engineering, CAS, Ningbo, 315000, China

[d] Wolong Electric Group Zhejiang Dengta Power Source Co., Ltd, Shaoxing, 312300, China

Material Synthesis

Synthesis of MWCNTs/Sn_4P_3: Typically, 100 mg MWCNTs/SnO_2 was hand-milled with 1 g NaH_2PO_2, and then heated at 300 °C for 30 min with a heating rate of 5 °C min^{-1} in Ar atmosphere. After the furnace was cooled down, the dark sample was obtained by washing the mixtures with water and HCl solution (0.1 M) for three times, respectively. Finally, the product was dried in a 60 °C vacuum oven for 12 h.

Synthesis of Sn_4P_3: In a typical procedure, amounts of Sn and red phosphorus with the molar ratio of 4:6 (Sn/P) were added into ethylenediamine solution and kept stirring for 3 h. Then the dispersion was transferred into a 50mL Teflon-lined autoclave and maintained at 200 °C for 40 h. Subsequently, the mixture was cooled down naturally. The samples were centrifuged with water and ethanol, respectively, followed by stirring in diluted HCl (0.1 mol L^{-1}) for 24 h. Then the mixture was washed with water and ethanol for several times and dried under vacuum at 60 °C.

[1] b*Corresponding author. Tel: +86-13670198451. E-mail: wangwenhui@hit.edu.cn
[2] a*Corresponding author. Tel: +86-0451-86413721. E-mail: changsd@hit.edu.cn

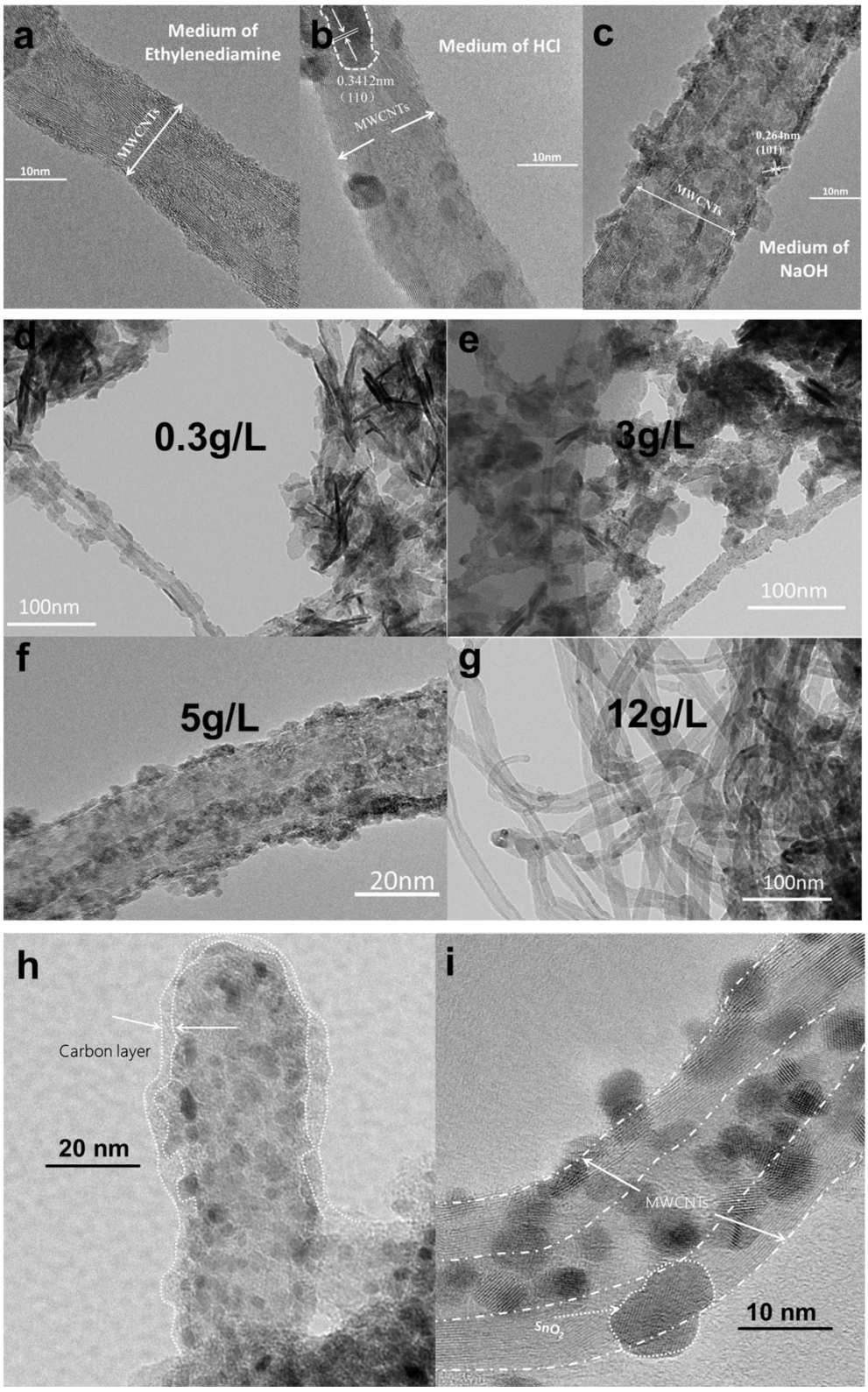

Figure S1. The influence of hydrothermal conditions on the synthesis of MWCNTs/SnO_2 composites. Effect of reaction media in hydrothermal reaction: (a) ethylenediamine, (b) HCl and (c) NaOH aqueous solution. Effect of MWCNTs concentration in hydrothermal reaction: (d) 0.3g L^{-1}; (e) 3g L^{-1}; (f) 5g L^{-1} and (g) 12g L^{-1} in the synthesis of MWCNTs/SnO_2 composites. Effect of calcination time on MWCNTs/SnO_2@C composites: (h) 2h and (i) 3h.

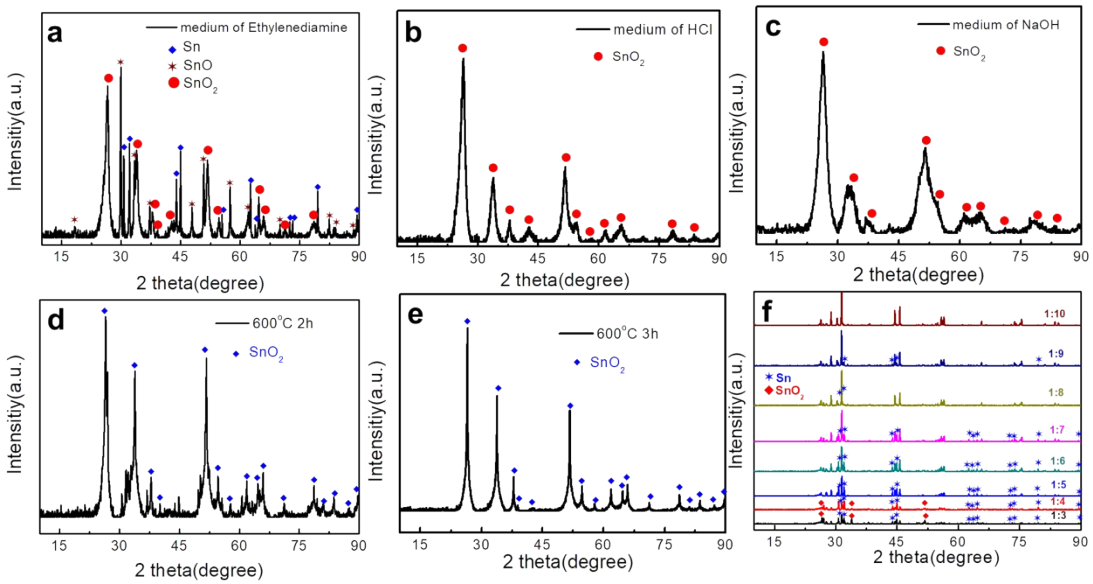

Figure S2. XRD patterns of MWCNTs/SnO_2 obtained under different synthetic conditions. Effect of reaction media in hydrothermal reaction: (a) ethylenediamine, (b) HCl and (c) NaOH aqueous solution. XRD patterns of MWCNTs/SnO_2@C composites. Effect of different calcination time: (d) 2h and (e) 3h. (f) XRD patterns of the MWCNTs/Sn_4P_3@C composites with different quality ratio (MWCNTs/SnO_2@C: NaH_2PO_2).

The synthesis procedures of MWCNTs/Sn_4P_3@C composites were described in detail in Figure S1-2, including the effect of medium, concentrations and calcination time on the required composition. Firstly, the medium of hydrothermal reaction was investigated, including ethylenediamine, HCl and NaOH. No SnO_2 nanoparticles is obviously observed on the surfaces of MWCNTs (Figure S1a) when ethylenediamine was used, while the corresponding XRD pattern (Figure S2a) exhibits diffraction peaks of SnO_2 phase. The result illustrates that Sn^{2+} mainly occurs hydrolysis reaction in aqueous solution. Rare nanoparticles were found on MWCNTs surface when HCl aqueous solution was used, while dense nanoparticles were anchored on the MWCNTs backbone when NaOH aqueous solution was used due to the reaction between Sn^{2+} ions and MWCNTs by means of electrostatic interaction (Figure S1b-c, S2b-c). The hydrolysis reaction is displayed as follows[1]: $Sn^{2+} + 2H_2O \leftrightarrow [Sn\cdot(H_2O)^2]^{2+} \leftrightarrow Sn(OH)^+ + H_3O^+$. According to the equation, Sn^{2+} ions transformed into $Sn(OH)^+$ ions due to the depletion of H_3O^+ ions in NaOH condition, and thus

easily attached to the surfaces of carboxyl-functionalized MWCNTs with negative charge[2]. Based on the above result, NaOH aqueous solution was chosen reaction medium for hydrothermal synthesis.

Subsequently, the effect of MWCNTs concentration on the as-synthesized MWCNTs/SnO_2 composites was investigated. The detailed architecture evolution of MWCNTs/SnO_2 composites are explicated in Figure S1d-g. It is showed that SnO_2 nanoparticles agglomerate at low concentration and rare SnO_2 nanoparticles dispersed at high concentration. Based on the above results, the MWCNTs/SnO_2 composites presented in the manuscript are obtained in the appropriate conditions, where the concentration of raw materials and MWCNTs were 5g L^{-1} and the reaction medium was NaOH aqueous solution.

In this paragraph, the synthesis parameters of carbonization process were investigated. Polydopamine (PDA) was selected as carbon sources. Firstly, the MWCNTs/SnO_2 precursor was mixed in PDA solution under magnetic stirring for about 24 h to ensure the uniform coating of PDA on MWCNTs/SnO_2. Secondly, the MWCNTs/SnO_2@PDA was subjected to annealing at 600 ^oC under Ar atmosphere to obtain MWCNTs/SnO_2@C. It is found that a uniform carbon layer had been decorated on the surface of MWCNTs/SnO_2 composites after being annealed for 2 h (Figure S1h, S2d), while the carbon layer disappeared when the annealing time was pro-long to 3 h (Figure S1i). Consequently, the best calcination time to obtain the carbon layer is 2 h.

Finally, the SnO_2 nanoparticles were chemically transformed into Sn_4P_3 nanoparticles by reacting with NaH_2PO_2. The mass ratio of MWCNTs/SnO_2@C and NaH_2PO_2 is of critical importance in the process as shown in Figure S2f. The SnO_2 nanoparticles are completely transformed into Sn_4P_3 nanoparticles when the mass

ratio of MWCNTs/SnO_2@C composites with NaH_2PO_2 reaches to 1:10.

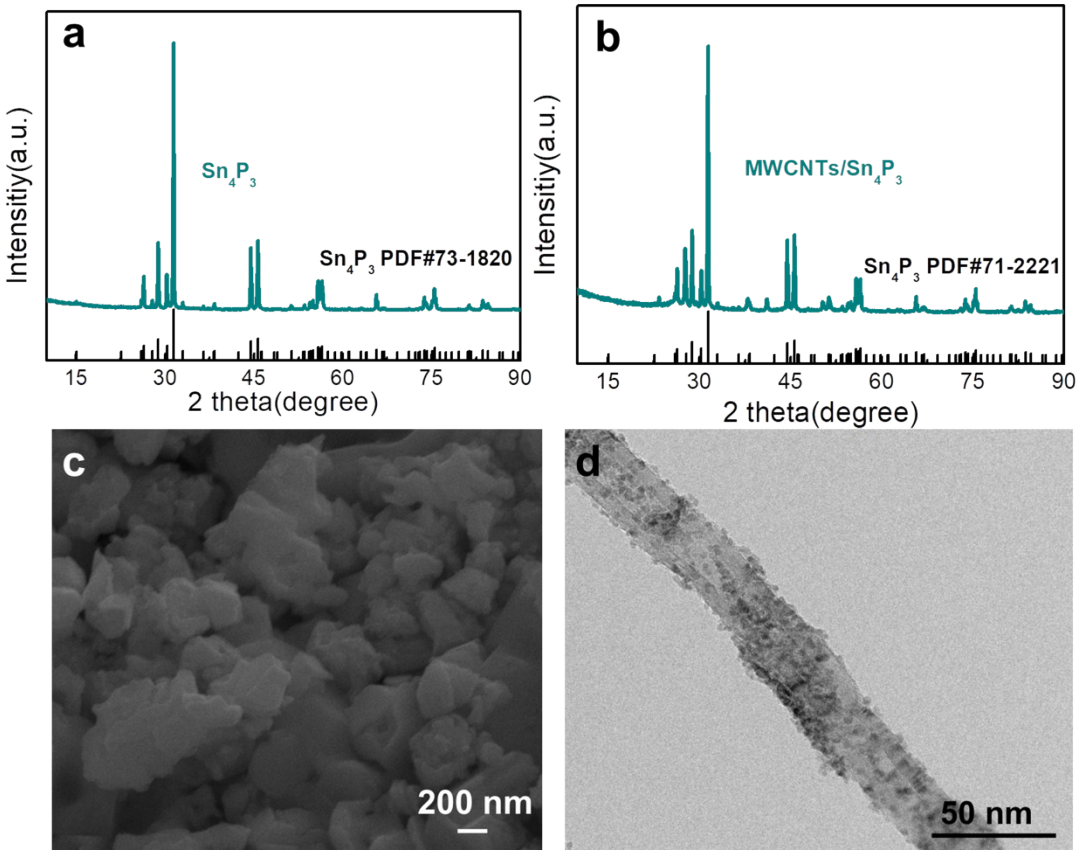

Figure S3. XRD patterns of the (a) bare Sn_4P_3 and (b) MWCNTs/Sn_4P_3. (c) SEM image of the bare Sn_4P_3. (d) TEM image of the MWCNTs/Sn_4P_3.

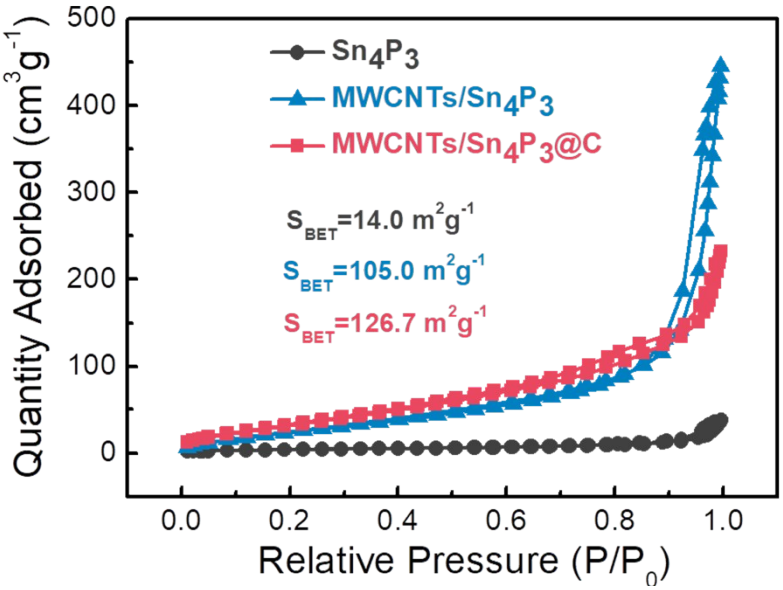

Figure S4. N_2 adsorption-desorption spectra of Sn_4P_3, MWCNTs/Sn_4P_3 and MWCNTs/Sn_4P_3@C.

Table S1 Carbon content of MWCNTs/SnO_2 and MWCNTs/Sn_4P_3@C.

Material	Carbon content(wt%)
MWCNTs/Sn_4P_3	26.04
MWCNTs/Sn_4P_3@C	32.51

Table S2 Electrical conductivity of Sn_4P_3 and MWCNTs/Sn_4P_3@C

Material	Electrical conductivity (S m^{-1})		
Sn_4P_3	1.72×10^{-4}	1.76×10^{-4}	1.76×10^{-4}
MWCNTs/Sn_4P_3	7.72×10^{-3}	7.19×10^{-3}	7.38×10^{-3}
MWCNTs/Sn_4P_3@C	7.52×10^{-2}	8.06×10^{-2}	8.20×10^{-2}

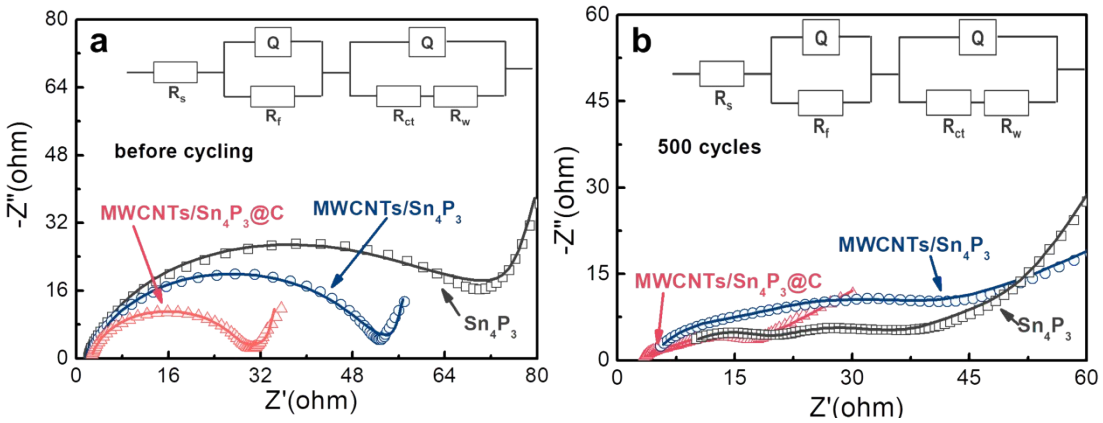

Figure S5. The Nyquist plots of bare Sn_4P_3, MWCNTs/Sn_4P_3 and the MWCNTs/Sn_4P_3@C electrodes. (a) before cycling; (b) after cycling 500 times at 500 mA g^{-1} (inset shows the equivalent circuit diagram).

The components for R_s, R_f and R_{ct} in the equivalent circuit diagram for the MWCNTs/Sn_4P_3@C electrode represent the electrolyte resistance, the SEI film resistance and charge-transfer resistance, respectively. Moreover, the inclined line in the low frequency region of the plots is relevant to the Warburg impedance (R_w), which represents the diffusion coefficient of Li^+ at the interface between the electrode and the electrolyte[3]. Based on a fitted equivalent circuit, the charge transfer resistances were obtained after 500 cycles at the full de-lithiated state.

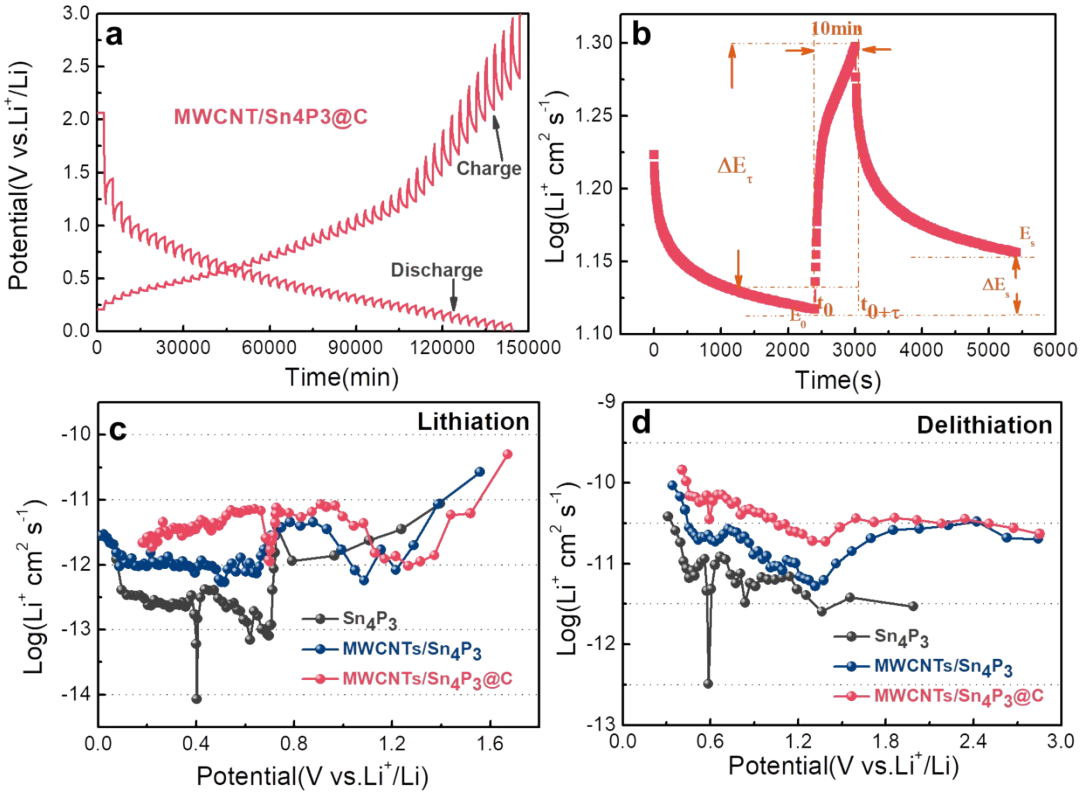

Figure S6. (a) The GITT curve of MWCNTs/Sn_4P_3@C during the charge/discharge process in 0.01-3.0 V. (b) The voltage profile for a single titration. The calculated Li^+ diffusion coefficients (D_{Li^+}) from GITT curves for Sn_4P_3, MWCNTs/Sn_4P_3 and MWCNTs/Sn_4P_3@C as a function of cell voltage during (c) the lithiation process and (d) the de-lithiation process.

The diffusion coefficients can be further quantified according to the following equation (Eq. (1))[4]:

$$D_{Li+} = \frac{4}{\pi\tau}\left(\frac{m_B V_M}{M_B A}\right)^2\left(\frac{\Delta E_S}{\Delta E_\tau}\right)^2 \qquad (1)$$

where V_M and m_B represent the molar volume of the compound and the mass of active material, respectively. The data of Sn_4P_3 were used in our calculation. In addition, M_B is relevant to the molecular weight and A indicates the total contact area between the electrolyte and the electrode. Generally, either the geometric electrode or the BET surface is used as an approximation of A[5], and the geometric surface area of the electrode was used in this paper. ΔEs represents the voltage difference of each intermittent step, and $\Delta E\tau$ is related with the change in the overall voltage under constant current conditions.

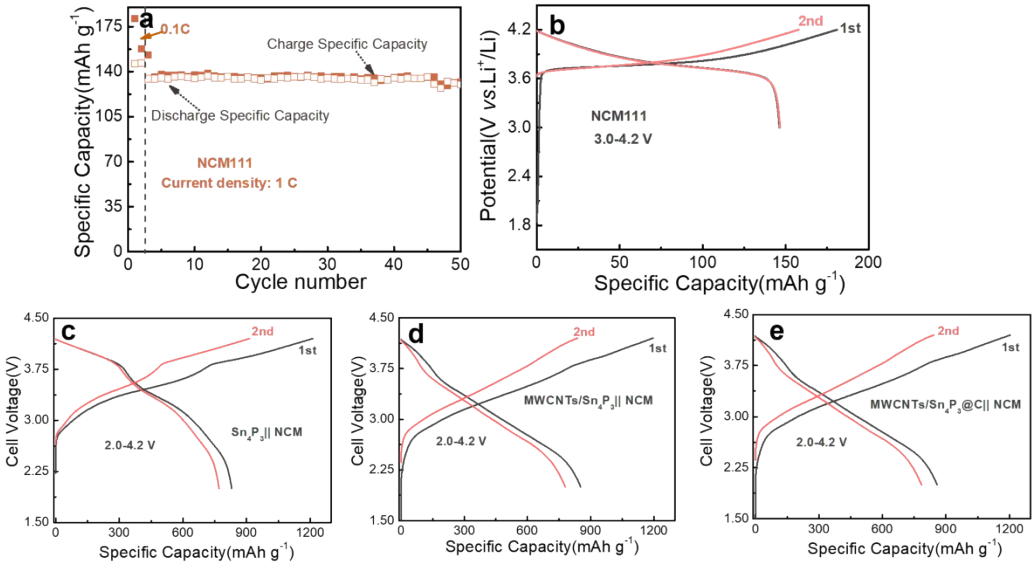

Figure S7. (a) The cycling performance curve of NCM111 half-cell at 3.0-4.3 V. Voltage profiles of the (b) NCM111 half cell at the current density of 0.1 C, (c) Sn_4P_3||NCM, (d) MWCNTs/Sn_4P_3||NCM and (e) MWCNTs/Sn_4P_3@C||NCM full cell at the current density of 200 mA g^{-1}.

References

1. H. Cox and A. J. Stace, Stace, Molecular View of the Anomalous Acidities of Sn^{2+}, Pb^{2+}, and Hg^{2+}. *J. Am. Chem. Soc.*, 2004, **126**, 3939-3947.

2. A. K. Jain, V. Dubey, N. K. Mehra, N. Lodhi, M. Nahar, D. K. Mishra and N. K. Jain, Carbohydrate-conjugated multiwalled carbon nanotubes: development and characterization. *Nanomedicine: Nanotechnology, Biology and Medicine*, 2009, **5**, 432-442.

3. Y. Von Lim, S. Huang, Y. Zhang, D. Kong, Y. Wang, L. Guo, J. Zhang, Y. Shi, T. P. Chen, L. K. Ang and H. Y. Yang, Bifunctional porous iron phosphide/carbon nanostructure enabled high-performance sodium-ion battery and hydrogen evolution reaction. *Energy Storage Materials*, 2018, **15**, 98-107.

4. J. W. Dibden, N. Meddings, J. R. Owen and N. Garcia Araez, Quantitative Galvanostatic Intermittent Titration Technique for the Analysis of a Model System with Applications in Lithium-Sulfur Batteries. *Chem. electrochem.*, 2018, **5**, 445-454.

5. H. Huang, T. Faulkner, J. Barker and M. Y. Saidi, Lithium metal phosphates, power and automotive applications. *J. Power Sources*, 2009, **189**, 748-751.